

RESEARCH ARTICLE | APRIL 05 2024

Prime number factorization with light beams carrying orbital angular momentum

Xiaofei Li; Xin Liu ; Quanying Wu ; Jun Zeng  ; Yangjian Cai  ; Sergey A. Ponomarenko ; Chunhao Liang  

 Check for updates

APL Photonics 9, 046107 (2024)

<https://doi.org/10.1063/5.0192223>



View
Online



Export
Citation



AIP Photonics
Special Topic: Brillouin Scattering
and Optomechanics
Submit Today

 AIP
Publishing

Prime number factorization with light beams carrying orbital angular momentum

Cite as: APL Photon. 9, 046107 (2024); doi: 10.1063/5.0192223
Submitted: 18 December 2023 • Accepted: 20 March 2024 •
Published Online: 5 April 2024



Xiaofei Li,^{1,2,3} Xin Liu,^{1,2}  Quanying Wu,^{4,a)} Jun Zeng,^{1,2,a)}  Yangjian Cai,^{1,2,a)}  Sergey A. Ponomarenko,^{3,5} 
and Chunhao Liang^{1,2,a)} 

AFFILIATIONS

- ¹ Shandong Provincial Engineering and Technical Center of Light Manipulation and Shandong Provincial Key Laboratory of Optics and Photonic Devices, School of Physics and Electronics, Shandong Normal University, Jinan 250014, China
- ² Collaborative Innovation Center of Light Manipulations and Applications, Shandong Normal University, Jinan 250358, China
- ³ Department of Electrical and Computer Engineering, Dalhousie University, Halifax, Nova Scotia B3J 2X4, Canada
- ⁴ Jiangsu Key Laboratory of Micro and Nano Heat Fluid Flow Technology and Energy Application, School of Physical Science and Technology, Suzhou University of Science and Technology, Suzhou 215009, China
- ⁵ Department of Physics and Atmospheric Science, Dalhousie University, Halifax, Nova Scotia B3H 4R2, Canada

^{a)} Authors to whom correspondence should be addressed: wqcyh@usts.edu.cn, zengjun@sdnu.edu.cn, yangjiancai@sdnu.edu.cn, and chunhaoliang@sdnu.edu.cn

ABSTRACT

We point out a link between orbital angular momentum (OAM) carrying light beams and number theory. The established link makes it possible to formulate and implement a simple and ultrafast protocol for prime number factorization by employing OAM endowed beams that are modulated by a prime number sieve. We are able to differentiate factors from non-factors of a number by simply measuring the on-axis intensity of light in the rear focal plane of a thin lens focusing on a source beam. The proposed protocol solely relies on the periodicity of the OAM phase distribution, and hence, it is applicable to fully as well as partially coherent fields of any frequency and physical nature—from optical or x-ray to matter waves—endowed with OAM. Our experimental results are in excellent agreement with our theory. We anticipate that our protocol will trigger new developments in optical cryptography and information processing with OAM beams.

© 2024 Author(s). All article content, except where otherwise noted, is licensed under a Creative Commons Attribution (CC BY) license (<https://creativecommons.org/licenses/by/4.0/>). <https://doi.org/10.1063/5.0192223>

The orbital angular momentum (OAM) beams have attracted enormous interest within the optical community since the pioneering work of Allen.^{1,2} Ever since their inception, the OAM beams have found diverse applications that take advantage of their phase singularities and mode orthogonality, among other unique properties. He *et al.* first observed the transfer of the optical OAM to a microparticle, causing particle trapping by an optical vortex around a phase singularity.³ Larocque *et al.* proposed the concept of optical framed topology, whereby the structures formed by the evolution of the phase singularity in space are employed as the information carriers to implement potent, high-security information encoding.^{4,5} Furthermore, optical vortices can be utilized for mode division multiplexing to realize ultra-high capacity optical

communication protocols.^{6,7} Fang *et al.* advanced OAM holography as a promising technique for high-security, high-capacity optical encryption.^{8–10}

On the other hand, the prime number decomposition of an integer, which is a cornerstone of number theory, has piqued the curiosity of the physics community due to recently discovered intriguing connections between number theory, condensed matter physics,¹¹ and photonics,¹² respectively. Factorizing a large integer into primes is a tricky problem, although. On the flip side, the complexity of the task can ensure high security for number-decomposition based information encoding, all-optical machine learning, and other number factorization related applications.^{5,13–15} To date, several approaches have been proposed to realize efficient

prime number decomposition,^{16–25} including quantum algorithms, quantum annealing, variational algorithms, and classical protocols involving Gauss sums. The latter involves coherent superpositions of optical waves,^{19,20} Bose–Einstein condensates,²¹ nuclear spins,²² cold atoms,²³ or matter waves in atom interferometers.²⁴ Interferometric approaches typically employ multiple sources to realize a Gauss sum, whereby a single source produces a term in the sum. Therefore, such techniques place strenuous demands on precise phase control of multiple wave sources, which is often difficult to implement in experiments, especially if factorizing a large number is required.²⁴ At the same time, the factorization procedure relying on the optical Talbot effect is hampered by light diffraction from the apertures of an optical system, which, ultimately, sets the upper limit on the factorizable number. Indeed, Pelka *et al.* were able to factor only a modest number of 27 using this approach.¹⁹ Recently, we have advanced a number factorization protocol employing axial correlation revivals of structured random waves, such that no phase control was necessary at all.²⁰ The approach of Ref. 20 makes it possible to decompose a number as large as a few million, but it is rather time-consuming to work with large statistical ensembles to accurately determine the speckle statistics.

In this work, we propose and implement a conceptually simple, time-efficient classical optical approach to number factorization that involves OAM carrying optical beams and a carefully engineered prime number sieve. Our approach relies on the intrinsic periodicity of the phase distribution of an optical OAM beam propagating in free space.

Consider the simplest OAM carrying optical beam, a Laguerre–Gaussian (LG) beam of zero radial mode index. The complex field amplitude of the beam can be expressed in cylindrical coordinates as²⁶

$$E_l(r, \varphi) = A_0 \left(\frac{\sqrt{2}r}{w_0} \right)^{|l|} \exp\left(-\frac{r^2}{w_0^2}\right) \exp(-il\varphi), \quad (1)$$

where l is a topological charge of the beam vortex and w_0 is a beam width at its waist. The phase of the beam field spirals around the beam propagation direction z , as schematically shown in Fig. 1(a). In any transverse plane $z = \text{const}$, the phase is manifestly periodic with the period $\varphi_T = 2\pi/|l|$, which is independent of the sign of the topological charge. In the following, we only consider the positive topological charge.

To perform prime number decomposition with such LG beams, we engineer a prime number sieve composed of M Dirac pinholes lying on a curve spiraling around the optical axis, as shown in Fig. 1(b). The transmittance function T_p of the sieve is defined as

$$T_p(r, \varphi) = \frac{1}{M} \sum_{m=1}^M \delta\left(\varphi - \frac{2\pi m^2}{p} + \varphi_0\right) \delta(r - r_m), \quad (2)$$

where M is the number of pinholes, δ is the Dirac delta function, and φ_0 denotes the initial phase. In the experiment, each Dirac pinhole is replaced by a circle of diameter d . Furthermore, $r_m = r_0 + m^2/p \cdot d$ is an offset of the m th pinhole from the optical axis; p is a trail factor, and m^2/p determines in between which consecutive rings the m th pinhole is located. The second delta function on the right-hand side of Eq. (2) ensures that the pinholes falling into the areas between different consecutive rings do not overlap.

We envision an optical system such that the OAM beam, modulated by the prime number sieve, is focused by a thin lens [see Fig. 1(c)] onto an observation screen. We can express the beam field in the rear focal plane of the lens as

$$U_f(\mathbf{r}) = -\frac{i}{\lambda f} \int d^2\mathbf{r}' E_l(\mathbf{r}', \varphi) T_p(\mathbf{r}', \varphi) e^{-ik\mathbf{r}' \cdot \mathbf{r}/f}, \quad (3)$$

where $\mathbf{r} = (r, \theta)$ and $\mathbf{r}' = (r', \varphi)$. By substituting Eqs. (1) and (2) into Eq. (3), we obtain

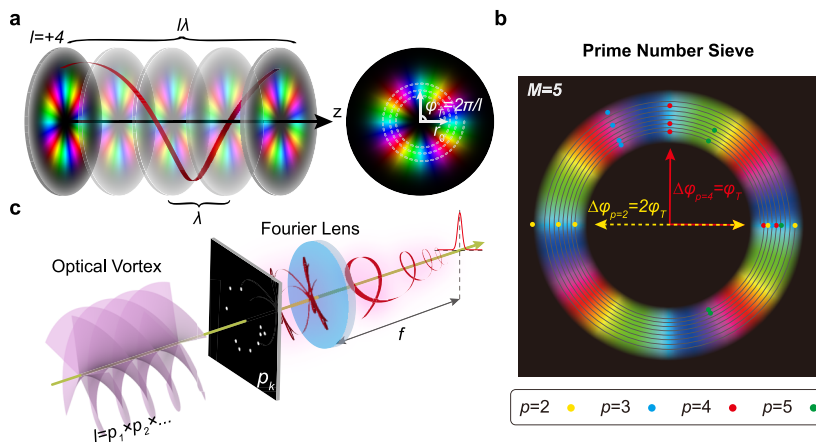


FIG. 1. Schematic illustration of the principle of prime number factorization with OAM beams. (a) The phase distribution of an OAM beam twisted as a spiral staircase during propagation exhibits azimuthal periodicity with the period $\varphi_T = 2\pi/l$. (b) Prime number sieve examples marked with color dots. (c) Implementing prime number factorization with OAM beams. The hue and brightness of the plots in (a) and (b) refer to the phase and intensity, respectively.

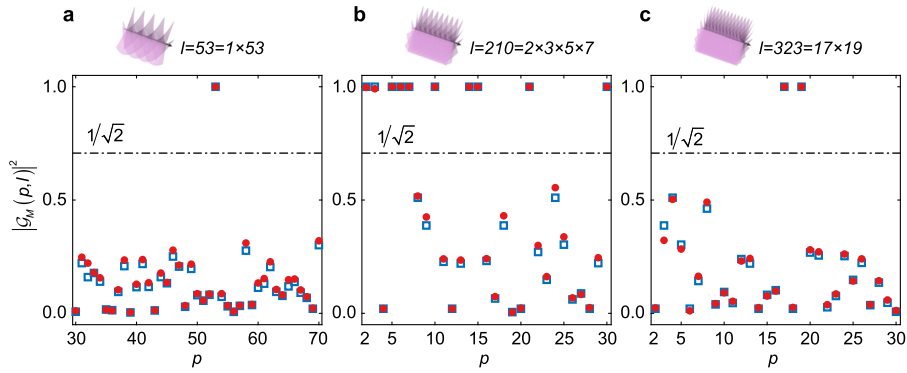


FIG. 2. Numerical simulation of prime number factorization with the OAM beam with $l = 1 \times 53$ (a), $l = 2 \times 3 \times 5 \times 7$ (b), and $l = 17 \times 19$ (c). The blue squares (red dots) mark theoretical results obtained from the incomplete Gauss sum (simulation results obtained with the aid of Matlab).

$$U_f(\mathbf{r}) \propto \frac{1}{M} \sum_{m=1}^M r_m \left(\frac{\sqrt{2} r_m}{w_0} \right)^{|l|} e^{-r_m^2/w_0^2} e^{-2\pi i \Delta\varphi_p/\varphi_T} \times \exp \left[-\frac{i k r r_m}{f} \cos \left(\theta - \frac{2\pi m^2}{p} + \varphi_0 \right) \right], \quad (4)$$

up to an immaterial constant. In the approximation $r_0 \gg m^2/p$, the on-axis intensity reduces to

$$I_{\text{axis}} \propto \left| \frac{1}{M} \sum_{m=1}^M \exp \left(-2\pi i \frac{\Delta\varphi_p}{\varphi_T} \right) \right|^2 = |\mathcal{E}_M(p, l)|^2, \quad (5)$$

where $\Delta\varphi_p = 2\pi m^2/p$. The function $\mathcal{E}_M(p, l)$ is an incomplete Gauss sum, defined as²⁵

$$\mathcal{E}_M(p, l) = \frac{1}{M} \sum_{m=1}^M \exp(-2\pi i m^2 l/p). \quad (6)$$

In our protocol, the number to be factored and the trial factors are given by the topological charge l of an OAM beam and the number p , which specifies the locations of the pinholes in the sieve. The Gauss sum equals unity whenever $\Delta\varphi_p$ are multiples of φ_T , such that p is a factor of the topological charge. Otherwise, $\mathcal{E}_M(p, l)$ oscillates rapidly, taking on small values. In Fig. 1(b), we exhibit four prime number sieves with $p = 2, 3, 4$, and 5 , marked by dots of different colors. We assume there are five pinholes, $M = 5$, and the number to be factorized is $l = 4$. Whenever p is a factor of l , i.e., $p = 2$ (yellow dots) and 4 (red dots), all pinholes are in phase. We can infer from Eq. (5) that the result is independent of the initial phase φ_0 , implying that our protocol is insensitive to the initial placement angle of the sieve. This is a huge bonus for the experimental implementation of our protocol. We note that we adopt a general criterion $M \geq 0.7\sqrt[4]{l}$ to suppress all non-factors situated below a threshold value $1/\sqrt{2}$ to improve factor identification.²⁵

We now present our numerical simulations of the proposed number factorization protocol sketched in Fig. 1(c). The incident OAM beam with the topological charge l and wavelength λ passes through the prime number sieve and is then focused by a thin lens

of focal length f . We can evaluate the on-axis intensity numerically using Matlab.²⁷ We chose the following numerical parameters: $\lambda = 532 \text{ nm}$, $f = 400 \text{ mm}$, $d = 0.04 \text{ mm}$, $r_0 = 6 \text{ mm}$, and $M = 7$. In Fig. 2, we display three examples of prime number factorization with OAM beams of variable l . We express the number l to be factorized as a product of prime factors, exhibited on top of each panel in Fig. 2. All results demonstrate that as long as p is a factor of l , the (normalized) on-axis intensity equals unity for good accuracy; otherwise, it takes on small values below the threshold value $1/\sqrt{2}$ labeled by the dashed-dotted line. Our theoretical results (blue squares, attained by the incomplete Gauss sum) and simulation results (red dots) are in good agreement, validating the feasibility of our protocol.

We proceed to the experimental implementation of the protocol. A linearly polarized beam of the carrier wavelength 532 nm , emitted from a DPSS laser, passes through a half-wave plate (HP) and a beam expander (BE). We rotate HP to guarantee the horizontal

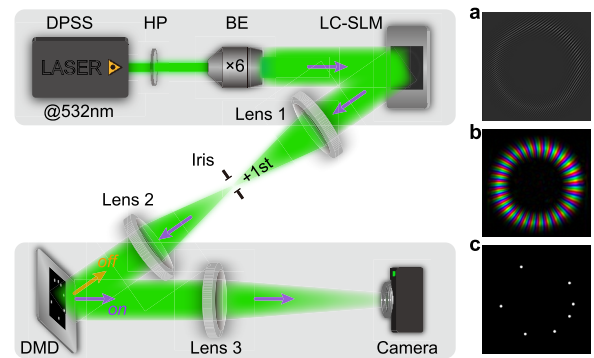


FIG. 3. Experimental setup for prime number factorization with OAM beams. DPSS: diode-pumped solid-state laser, HP: half-wave plate, BE: beam expander, SLM: reflective phase-only liquid crystal spatial light modulator, and DMD: digital micro-mirror device. (a) Computer-generated hologram of a Laguerre-Gauss beam with topological charge $l = 30$ and $w_0 = 0.8 \text{ mm}$. (b) Complex amplitude of an experimentally reproduced Laguerre-Gaussian beam at the front surface of the DMD. The image size is $9.6 \times 9.6 \text{ mm}^2$, and hue and brightness refer to the phase and intensity, respectively. (c) An example mask of prime number sieve T_p with $M = 7$, $d = 0.15 \text{ mm}$, and $r_0 = 3 \text{ mm}$.

polarization of an output beam, as it must align with the reflection angle of a phase-only spatial light modulator (SLM) (Holoeye GAEA-2, 3840×2160 pixels with a $3.74 \times 3.74 \mu\text{m}^2$ pixel pitch). To generate a high-quality OAM beam [described by Eq. (1)], we employ the complex-amplitude encoding scheme²⁶ to customize a computer-generated hologram to be loaded onto the SLM [see an example for $l = 30$ in Fig. 3(a)]. The input beam illuminates the SLM, and the +first or -first-order diffracted beam forms our output OAM beam. Such a beam can be selected via a modified $4f$ optical system consisting of two lenses of focal length $f_1 = f_2 = 10$ cm and an iris. We employ a generalized Arago spot method²⁸ to obtain the complex field distribution of the generated OAM beam, which we illustrate in Fig. 3(b). Hue and brightness refer to the phase and intensity of the beam, respectively. The generated OAM beam illuminates a Digital Micro-mirror Device (DMD) (Vialux, 1920×1080 pixels with a $10 \times 10 \mu\text{m}^2$ pixel pitch), on which the prime number sieve is loaded. The sieve is displayed in Fig. 3(c), and the relevant parameters are set as $M = 7$, $d = 0.15$, mm and $r_0 = 3$ mm. The modulated beam is focused by a thin lens (lens 3) of a focal length of $f_3 = 40$ cm, and a camera, located in the rear focal plane of the lens, records an intensity pattern.

We exhibit three normalized intensity patterns in Fig. 4. We take the topological charge to be $l = 30$. Following Eq. (2), we design three prime number sieves, varying the magnitude of p . We set the other parameters as $M = 7$, $d = 0.15$ mm, and $r_0 = 3$ mm. We find that the on-axis normalized intensity (marked by the cross symbol) is unity if p is a factor of $l = 30$ (see $p = 5$ and 10 in the central and right panels), or not (see $p = 4$ in the left panel). Furthermore, we experimentally factor the numbers $l = 30$ and $l = 53$. We present our results in Fig. 5. It can be seen in the figure that the factors and non-factors of both numbers are clearly discriminated by the threshold value of $1/\sqrt{2}$. Slight deviations of the experimental results from the simulation results are mainly due to misalignment between the OAM beam and prime number sieve axes, as well as to imperfect generation of the OAM beam. Overall, our experimental results agree well with our simulations, as shown in Figs. 4 and 5.

In our time-efficient number factorization protocol, l serves as a number to be factored, so that we first produce the required OAM beam. It is followed by the design of a set of variable trial number sieves. It is worth noting that the transmittance function of any sieve

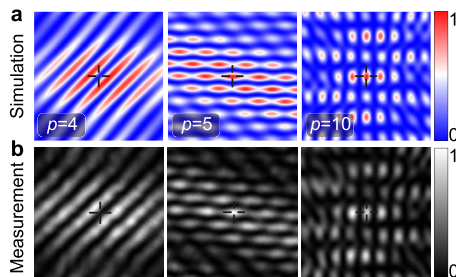


FIG. 4. Numerical (a) and experimental (b) results for the normalized intensity patterns of an OAM beam modulated by prime number sieves. The topological charge is $l = 30$, and the trial factor p is given by 4, 5, and 10 from left to right. The size of each pattern is $375 \times 375 \mu\text{m}^2$, and the optical axis is labeled by the cross symbol.

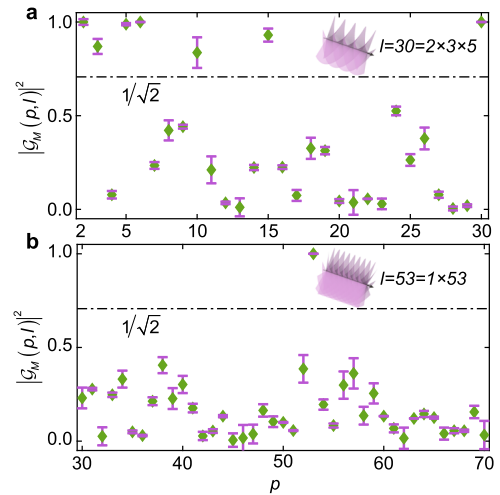


FIG. 5. Experimental implementation of prime number factorization with OAM beams. The number to be factorized is given by $l = 30$ (a) and $l = 53$ (b). The vertical lengths of the error bars characterize the absolute value of the difference between the experimental and simulation results.

is binary, such that light passes through the pinholes and is reflected otherwise. Such a sieve is realized by the DMD, and in the binary regime, the refreshment rate of the DMD can reach the maximum value of around 17 kHz. It implies that we can rapidly change the sieve in order to swiftly refresh the trial factor p . In the receiver plane, we can use the camera with a high frame rate to quickly record the intensity patterns of the modulated OAM beams, saved as 8-bit grayscale pictures. The commercial software Matlab reads a picture and converts it into a matrix. We save a gray value of the central pixel (corresponding to the on-axis intensity value) and plot it as a function of the trial number p . This function is normalized by its maximum to ensure the on-axis intensity value is unity when p is a factor of l . We can visually separate factors from non-factors by

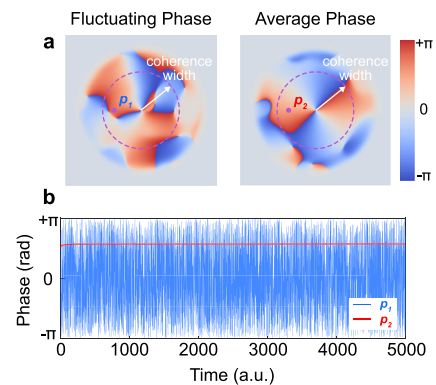


FIG. 6. (a) Fluctuating and ensemble average phases of the field of a noisy OAM beam. (b) Time evolution of two phases at the same locations within the phase distribution marked by the purple dots (p_1 and p_2) in (a). The radius of the purple dashed circles in (a) corresponds to the coherence width of the beam.

looking at the threshold line. According to the short board principle, the speed of our technology mainly depends on the lower refresh rate of the DMD and the camera frame rate. Here, we choose the camera (IBTEK, STC-MBS43POE) as an example. Its frame rate can be up to 282 fps, so the ideal time interval to test a trial factor is around 3.55 ms. If we attempt to factorize a large number $l = 10^6$, say, the trial factor p takes one value from 2 to \sqrt{l} . The total time it takes to perform the factorization is then around 3.55 s, which is significantly faster than the competing number factorization methods.

Furthermore, the noisy nature of any realistic light source implies that any genuine light beam is, in practice, only partially coherent. The latter has a random (fluctuating) phase. Our protocol heavily relies on the tight control of the source OAM beam and sieve pinhole phases and, hence, can lose credibility in the presence of phase fluctuations. To elucidate the role of phase fluctuations, we compare the fluctuating and ensemble average phases in Fig. 6(a). The latter is obtained by averaging over an ensemble of 5000 realizations of OAM beams with a topological charge of $l = 2$. We observe in the figure that the average phase is rather stable within the purple dashed circle area. In Fig. 6(b), we plot the phase magnitudes at the same locations, labeled by the purple dots p_1 and p_2 , within the phase distributions of the random and average phases. We can infer from the figure that the random phase (blue line) fluctuates dramatically with time, while the average phase (red line) is nearly stationary. Instructively, the average phase outside the purple dashed circle area fluctuates as well [see the right panel in Fig. 6(a)]. The radius of the circle is given by the coherence width of the source. Thus, we can employ noisy OAM beams in our number factorization protocol as long as the pinholes of the sieve are offset from the optical axis by distances shorter than the coherence width of the beam.

In summary, we have pointed out the link between number theory and the OAM beams that make it possible to formulate a simple and time-efficient protocol for number factorization. In our protocol, an OAM beam, modulated by a prime-number sieve, is focused by a thin lens. The number to be factorized corresponds to the topological charge of the beam, and all trials p are encapsulated into the sieve. The factors and non-factors can be distinguished by measuring the on-axis intensity of the focused beam. The experimental scheme is simple, and the results are independent of the sieve orientation. We can swiftly refresh a sieve with a DMD to change the trial factor p . In principle, we can decompose a number as large as 10^6 in 3.55 s by our protocol. For the upper bound on the number to be composed, we should realize the central angle (equal to d/r_0) corresponding to a circle is much smaller than the phase period $\varphi_T = 2\pi/l$, to ensure the Dirac pinhole can be replaced by a small-sized circle of diameter d . It is obtained by $l \ll 2\pi r_0/d$.

Our protocol works for noisy OAM beams as long as the sieve size is smaller than the coherence width of the beam. Our results are independent of the wavelength of light and only depend on the azimuthal periodicity of the phase distribution of OAM beams. Hence, our protocol is capable of handling any OAM beams, such as Laguerre–Gaussian, Bessel, etc., as well as vortex carrying waves of any physical nature (electron, matter-wave vortices, etc.).

Our work is able to serve for OAM detection, as we can determine all prime numbers of the OAM beam's topological charge value. Furthermore, we believe this advanced protocol can stimulate the development of optical encryption and encoding.^{4,5}

This work was supported by the National Key Research and Development Program of China (Grant Nos. 2022YFA1404800 and 2019YFA0705000), the National Natural Science Foundation of China (Grant Nos. 12374311, 11974218, 12104264, and 92250304), the Taishan Scholars Program of Shandong Province (Grant No. tsqn202312163), the Qingchuang Science and Technology Plan of Shandong Province (Grant No. 2022KJ246), the China Postdoctoral Science Foundation (Grant No. 2022T150392), the Natural Science Foundation of Shandong Province (Grant Nos. ZR2021QA014 and ZR2023YQ006), and the Natural Sciences and Engineering Research Council of Canada (Grant No. RGPIN-2018-05497).

AUTHOR DECLARATIONS

Conflict of Interest

The author has no conflicts to disclose.

Author Contributions

X.F.L. and X.L. contributed equally to this work.

X.L. and C.H.L. conceived the idea for the project and derived the theoretical model. X.L. and X.F.L. performed all simulations and experiments. X.F.L. and Q.Y.W. completed data acquisition. C.H.L., J.Z. and S.A.P. conducted the analysis and prepared the manuscript. C.H.L., Q.Y.W. and Y.J.C. supervised the work. All authors contributed to the analysis of the results and the writing of the paper and have accepted responsibility for the entire content of this manuscript and approved its submission.

Xiaofei Li: Data curation (equal); Formal analysis (equal); Investigation (equal); Methodology (equal). **Xin Liu:** Conceptualization (equal); Formal analysis (equal); Investigation (equal); Methodology (equal); Writing – original draft (equal). **Quanying Wu:** Formal analysis (equal); Project administration (equal); Validation (equal). **Jun Zeng:** Methodology (equal); Validation (equal); Writing – review & editing (equal). **Yangjian Cai:** Funding acquisition (equal); Project administration (equal); Supervision (equal). **Sergey A. Ponomarenko:** Investigation (equal); Project administration (equal); Writing – review & editing (equal). **Chunhao Liang:** Conceptualization (equal); Funding acquisition (equal); Supervision (equal); Writing – original draft (equal).

DATA AVAILABILITY

The data that support the findings of this study are available from the corresponding author upon reasonable request.

REFERENCES

- 1L. Allen, M. W. Beijersbergen, R. J. C. Spreeuw, and J. P. Woerdman, "Orbital angular momentum of light and the transformation of Laguerre–Gaussian laser modes," *Phys. Rev. A* **45**(11), 8185 (1992).
- 2Y. Shen, X. Wang, Z. Xie, C. Min, X. Fu, Q. Liu, M. Gong, and X. Yuan, "Optical vortices 30 years on: OAM manipulation from topological charge to multiple singularities," *Light: Sci. Appl.* **8**(1), 90 (2019).

- ³H. He, M. E. J. Friese, N. R. Heckenberg, and H. Rubinsztein-Dunlop, "Direct observation of transfer of angular momentum to absorptive particles from a laser beam with a phase singularity," *Phys. Rev. Lett.* **75**(5), 826 (1995).
- ⁴H. Larocque, A. D'Errico, M. F. Ferrer-Garcia, A. Carmi, E. Cohen, and E. Karimi, "Optical framed knots as information carriers," *Nat. Commun.* **11**(1), 5119 (2020).
- ⁵L. Kong, W. Zhang, P. Li, X. Guo, J. Zhang, F. Zhang, J. Zhao, and X. Zhang, "High capacity topological coding based on nested vortex knots and links," *Nat. Commun.* **13**(1), 2705 (2022).
- ⁶J. Wang, J. Yang, I. M. Fazal, N. Ahmed, Y. Yan, H. Huang, Y. Ren, Y. Yue, S. Dolinar, M. Tur, and A. E. Willner, "Terabit free-space data transmission employing orbital angular momentum multiplexing," *Nat. Photonics* **6**(7), 488–496 (2012).
- ⁷J. T. Barreiro, T. C. Wei, and P. G. Kwiat, "Beating the channel capacity limit for linear photonic superdense coding," *Nat. Phys.* **4**(4), 282–286 (2008).
- ⁸X. Fang, H. Ren, and M. Gu, "Orbital angular momentum holography for high-security encryption," *Nat. Photonics* **14**(2), 102–108 (2020).
- ⁹L. Kong, Y. Sun, F. Zhang, J. Zhang, and X. Zhang, "High-dimensional entanglement-enabled holography," *Phys. Rev. Lett.* **130**(5), 053602 (2023).
- ¹⁰H. Ren, X. Fang, J. Jang, J. Bürger, J. Rho, and S. A. Maier, "Complex-amplitude metasurface-based orbital angular momentum holography in momentum space," *Nat. Nanotechnol.* **15**(11), 948–955 (2020).
- ¹¹G. Mussardo, A. Trombettoni, and Z. Zhang, "Prime suspects in a quantum ladder," *Phys. Rev. Lett.* **125**(24), 240603 (2020).
- ¹²F. Sgrignuoli, S. Gorsky, W. A. Britton, R. Zhang, F. Riboli, and L. Dal Negro, "Multifractality of light in photonic arrays based on algebraic number theory," *Commun. Phys.* **3**(1), 106 (2020).
- ¹³H. Li, S. Fang, B. M. T. Lin, and W. Kuo, "Unifying colors by primes," *Light: Sci. Appl.* **12**(1), 32 (2023).
- ¹⁴X. Lin, Y. Rivenson, N. T. Yardimci, M. Veli, Y. Luo, M. Jarrahi, and A. Ozcan, "All-optical machine learning using diffractive deep neural networks," *Science* **361**(6406), 1004–1008 (2018).
- ¹⁵R. L. Rivest, A. Shamir, and L. Adleman, "A method for obtaining digital signatures and public-key cryptosystems," *Commun. ACM* **21**(2), 120–126 (1978).
- ¹⁶L. M. K. Vandersypen, M. Steffen, G. Breyta, C. S. Yannoni, M. H. Sherwood, and I. L. Chuang, "Experimental realization of Shor's quantum factoring algorithm using nuclear magnetic resonance," *Nature* **414**(6866), 883–887 (2001).
- ¹⁷X. Peng, Z. Liao, N. Xu, G. Qin, X. Zhou, D. Suter, and J. Du, "Quantum adiabatic algorithm for factorization and its experimental implementation," *Phys. Rev. Lett.* **101**(22), 220405 (2008).
- ¹⁸E. Anschuetz, J. Olson, A. Aspuru-Guzik, and Y. Cao, "Variational quantum factoring," in *Quantum Technology and Optimization Problems*, edited by S. Feld and C. Linnhoff-Popien (Springer, Cham, 2019), pp. 74–85.
- ¹⁹K. Pelka, J. Graf, T. Mehringer, and J. von Zanthier, "Prime number decomposition using the Talbot effect," *Opt. Express* **26**(12), 15009–15014 (2018).
- ²⁰X. Liu, C. Liang, Y. Cai, and S. A. Ponomarenko, "Axial correlation revivals and number factorization with structured random waves," *Phys. Rev. Appl.* **20**, L021004 (2023).
- ²¹M. Sadgrove, S. Kumar, and K. Nakagawa, "Enhanced factoring with a Bose–Einstein condensate," *Phys. Rev. Lett.* **101**(18), 180502 (2008).
- ²²M. Mehring, K. Müller, I. S. Averbukh, W. Merkel, and W. P. Schleich, "NMR experiment factors numbers with Gauss sums," *Phys. Rev. Lett.* **98**(12), 120502 (2007).
- ²³M. Gilowski, T. Wendrich, T. Müller, C. Jentsch, W. Ertmer, E. M. Rasel, and W. P. Schleich, "Gauss sum factorization with cold atoms," *Phys. Rev. Lett.* **100**(3), 030201 (2008).
- ²⁴D. Bigourd, B. Chatel, W. P. Schleich, and B. Girard, "Factorization of numbers with the temporal Talbot effect: Optical implementation by a sequence of shaped ultrashort pulses," *Phys. Rev. Lett.* **100**(3), 030202 (2008).
- ²⁵M. Štefaňák, W. Merkel, W. P. Schleich, D. Haase, and H. Maier, "Factorization with Gauss sums: Scaling properties of ghost factors," *New J. Phys.* **9**(10), 370 (2007).
- ²⁶X. Liu, Y. E. Monfared, R. Pan, P. Ma, Y. Cai, and C. Liang, "Experimental realization of scalar and vector perfect Laguerre–Gaussian beams," *Appl. Phys. Lett.* **119**(2), 0211205 (2021).
- ²⁷J. D. Schmidt, *Numerical Simulation of Optical Wave Propagation with Examples in MATLAB* (SPIE, Bellingham, 2010).
- ²⁸X. Liu, Q. Chen, J. Zeng, Y. Cai, and C. Liang, "Measurement of optical coherence structures of random optical fields using generalized Arago spot experiment," *Opto-Electron. Sci.* **2**(2), 220024 (2023).